Hindawi
Advances in Civil Engineering
Volume 2019, Article ID 8921502, 10 pages
https://doi.org/10.1155/2019/8921502

Research Article

Fire Behavior of the Assembled Monolithic Hollow-Ribbed Slabs

B. Li,[1] **Y. Q. Lin**,[1] **H. L. Zhang**,[2] **and M. J. Ma**[2]

[1]*College of Civil Engineering and Architecture, Hainan University, Haikou 570228, China*
[2]*Shandong Provincial Key Laboratory of Appraisal and Retrofitting in Building Structures, Shandong Jianzhu University, Jinan 250101, China*

Correspondence should be addressed to B. Li; tingchao136@vip.163.com

Received 19 March 2019; Accepted 20 August 2019; Published 8 October 2019

Academic Editor: Venu G. M. Annamdas

This paper presents the results from the furnace tests conducted on two assembled monolithic hollow-ribbed (AMH) slabs consisting of the open box and the covered box, respectively. Detailed experimental data in the form of describing slab cracking or spalling, furnace temperatures, temperature distributions, and vertical deflections are presented. Comparison of the results from the two fire tests indicates that the covered box shows better fire resistance compared to the open box; thus, the covered box is recommended to adopt in structural fire-resistant design. However, they are both prone to cracking or spalling at their bottom surfaces during the fire tests, so the AMH slab still needs further optimum design to meet its requirements of fire resistance and service function. In addition, the sealing quality of congruent boxes also has a great influence on the fire resistance of the AMH slab.

1. Introduction

The AMH slab floor is developed from the traditional ribbed floor and the cast-in-situ concrete hollow floor. As shown in Figure 1, it consists of prefabricated congruent boxes, cast-in-place concrete ribbed girders, and edge girders. As an important innovation of the slab structure field, it combines many advantages of two traditional floor structure systems and at the same time has solved many problems of the traditional floor. Furthermore, the AMH slab has the characteristics of light weight, little material, good integrity, and spatial performance and so on; thus, it can be used widely in large span, big space, or high-load buildings [1, 2].

At present, the AMH slab has been widely used in China. This has attracted some scholars to study its mechanical performance and construction technology [3–9]. Zhao et al. pointed out flexural failure occurs in the AMH slab, and the ribbed girders can be simplified as T-shaped bending members based on the experiment [3]. Zhou et al. [4] pointed out that the prefabricated top and side plates of the hollow box have a good bond with cast-in-situ concrete ribs, and then a new computational method for the calculation of stiffness and deformation which can yield more accurate and reasonable results was proposed. Shen and Zhu [5] tested a vast scale model of four sides simply supported reinforced concrete waffle floor slab and developed its simple ultimate loading formula. In the meantime, the deformation monitoring, seismic performance, dynamic identification, shear resistance, and so on were also discussed [6–9]. However, the effect of elevated temperature on the AMH slab has hardly been involved.

Fire is a disaster that frequently happens in buildings. Since the AMH floor slabs are gradually used in buildings and may be sensitive to fire, the influence of high temperature on their behavior should be studied further. In recent years, considerable research work has been conducted to study the performance of conventional reinforced concrete slabs, which could give some useful information to understand the fire behavior of the AMH slab tested on the presented experimental campaigns. Bailey and Toh [10] focused on the comparison between the behavior of small-scale reinforced slabs at ambient and elevated temperatures.

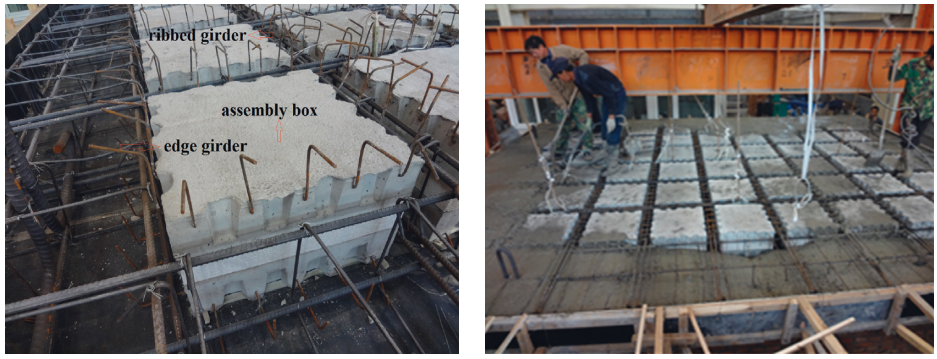

(a) (b)

Figure 1: View of the AMH floor. (a) Before pouring concrete. (b) Pouring concrete.

Dong and Zhu [11] reported the full-scale two-way concrete slabs under different support conditions in actual engineering and presented an equilibrium method considering tension membrane effects. Moss et al. [12] quantified the thermal deformations of two-way concrete slabs in a multistorey multibay building. Li et al. [13–15] performed similar analysis on two-way concrete slabs in a full-scale three-storey steel-framed building. Kakogiannis et al. [16] worked on the analysis of the blast bearing capacity of reinforced concrete hollow core slabs when they are subjected first to fire and then to a blast load. However, the differences between the AMH slab and conventional reinforced concrete slabs imply that whether the above test results can be applied to the AMH slab is still to be examined. In order to improve the knowledge of the performance of the AMH slab in fire conditions, two furnace tests were conducted on the AMH slabs with four-edge simple supports under the combined effects of constant loading and fire. In the meantime, the fire resistance behavior of the AMH slabs was discussed and feasible actions of improving the performance of fire resistance were put forward.

2. Test Program

2.1. Furnace Construction and Loading. Two tests were conducted on a specially designed furnace at Shandong Jianzhu University, China. As shown in Figure 2, the furnace was located underneath the test panels, and the heated slabs served as the upper cover of the furnace. The underside of the slab was heated by six oil-fired burner nozzles, which was located in the furnace walls symmetrically, and each nozzle was controlled independently from each other. Four Type S thermocouples were installed (two in each side shown in Figure 2(b)) to measure the temperatures of the gas inside the furnace.

During the fire tests, sandbags were placed on the slabs to simulate the uniformly distributed load of 2.0 KN/m^2 in addition to the self-weight [17], and the slabs were loaded at least two hours before each fire test, as shown in Figure 3(a). These sandbags were insulated from the upper surface of the test slab with wooden supports to avoid being damaged by high temperatures.

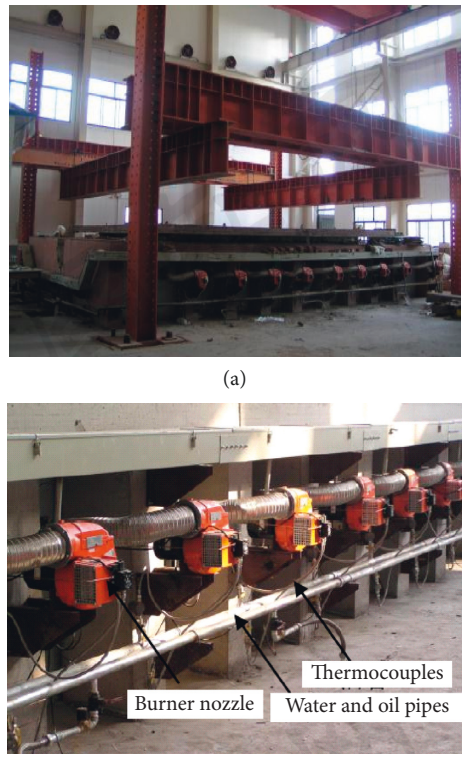

(a)

(b)

Figure 2: Picture of the furnace. (a) Complete picture. (b) Construction details.

According to the standard of concrete testing methods of China, the two slabs were both simply supported at all four sides above the furnace, as shown in Figure 3(b). The diameters of both steel balls and steel rollers of the simple edge supports were all 100 mm. There were 120 mm wide and 12 mm thick steel strips continuously between concrete slabs and steel balls or rollers, and the same steel strips were also arranged between steel balls or rollers and four reinforced concrete walls.

2.2. Sample Preparation for Fire Tests. In practice, some prefabricated congruent boxes are arranged in the AMH

(a) (b)

Figure 3: View of the loading. (a) Sandbags. (b) Supports.

slabs according to design schemes. They participate carrying the load with the ribbed girders and edge girders and can be used as the side template of girders when casting concrete. Generally, the section height of the congruent box can be chosen from 250 mm to 1400 mm according to the span and design load. Each congruent box consists of a soleplate, a top plate, and a rectangular frame plate. The plane sizes (mm) of the soleplates and top plates include 1000×1000, 1000×700, 1000×500, 700×700, 500×500, and so on, and their thickness can be chosen according to practical needs. In addition, the thickness of the frame plate can be chosen from 8 mm to 12 mm.

As shown in Figure 4, both the test AMH slabs have a size of 4800 mm × 6680 mm and the clear span is 4300 mm × 6180 mm. The actual heating span is assumed to be 3800 mm × 5680 mm, which also is the opening size of the furnace.

In each test slab 54 (6×9) congruent boxes are arranged. The congruent boxes can be classified as open boxes (Figure 5(a)) and covered boxes (Figure 5(b)). The open box has a target thickness of 300 mm, while the covered box has a target thickness of 350 mm because of additional 50 mm thick cast-in-situ layer at its top surface. The first testing AMH slab was made from open boxes, and the second testing AMH slab was made from covered boxes. Each congruent box has a plane size of 500 mm × 500 mm, and its soleplate and top plate are both 40 mm thick and reinforced by low-carbon steel wires (4 mm diameter) which are arranged at a spacing of 150 mm along both directions. The rectangular frame plate is 40 mm thick without reinforcement and can be used as side templates when casting concrete. The aforementioned subcomponents were all prefabricated at factory, and the specified compressive strength was 40 MPa. Furthermore, the ribbed girders BL and edge girders BLl–BL3, as shown in Figure 4, were casted-in-situ, and the specified compressive strength was 30 MPa. The detailed constructions of the aforementioned girders are illustrated in Figure 5. They were all reinforced with grade three hot-rolled reinforcing bars with a characteristic yield strength of 400 MPa. The actual yield and ultimate tensile strength are 426 and 573 MPa, respectively.

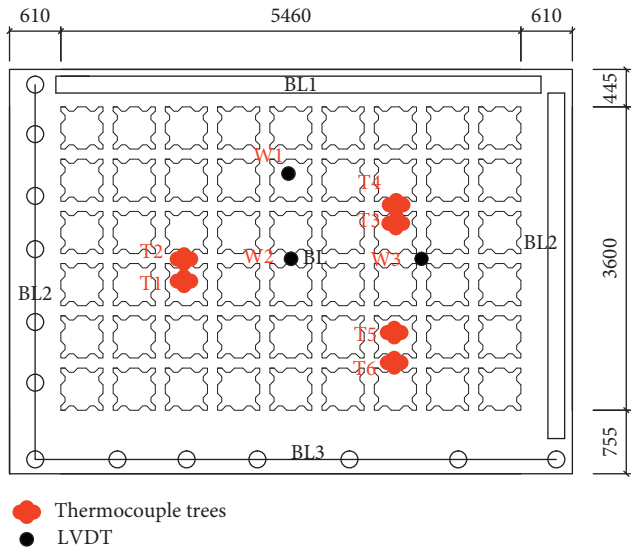

Figure 4: Structural plan dimension (mm).

3. Test Results and Discussion

3.1. Testing Phenomenon. Some testing phenomenons observed during the first fire test were recorded as shown in Figure 6. At 5 min after ignition, the test slab began popping noise due to crack propagation, and some water marks occurred on the surface of edge girders due to the evaporation of moisture and water migration. At 8 min, some soleplates of open boxes began to generate surface spalling. At 15 min, the flame has burned through most of the soleplates and entered into their interior. Meanwhile, the test slab fluctuated obviously. At 35 min, the four corners of the test slab began to deflect vertically upward, and correspondingly the steel balls at the corners had lost their supporting role. At 69 min, the top plate of an open box was burned through; thus, the flame emerged from the cracks. At 90 min, the open boxes had been burned through in many places, which obviously did not meet the requirements of the first-order fire-resistant grade of the floor slab [18]. After the fire test, the fired concrete of the soleplates turned white and fell off seriously. But the lateral plates appeared to have

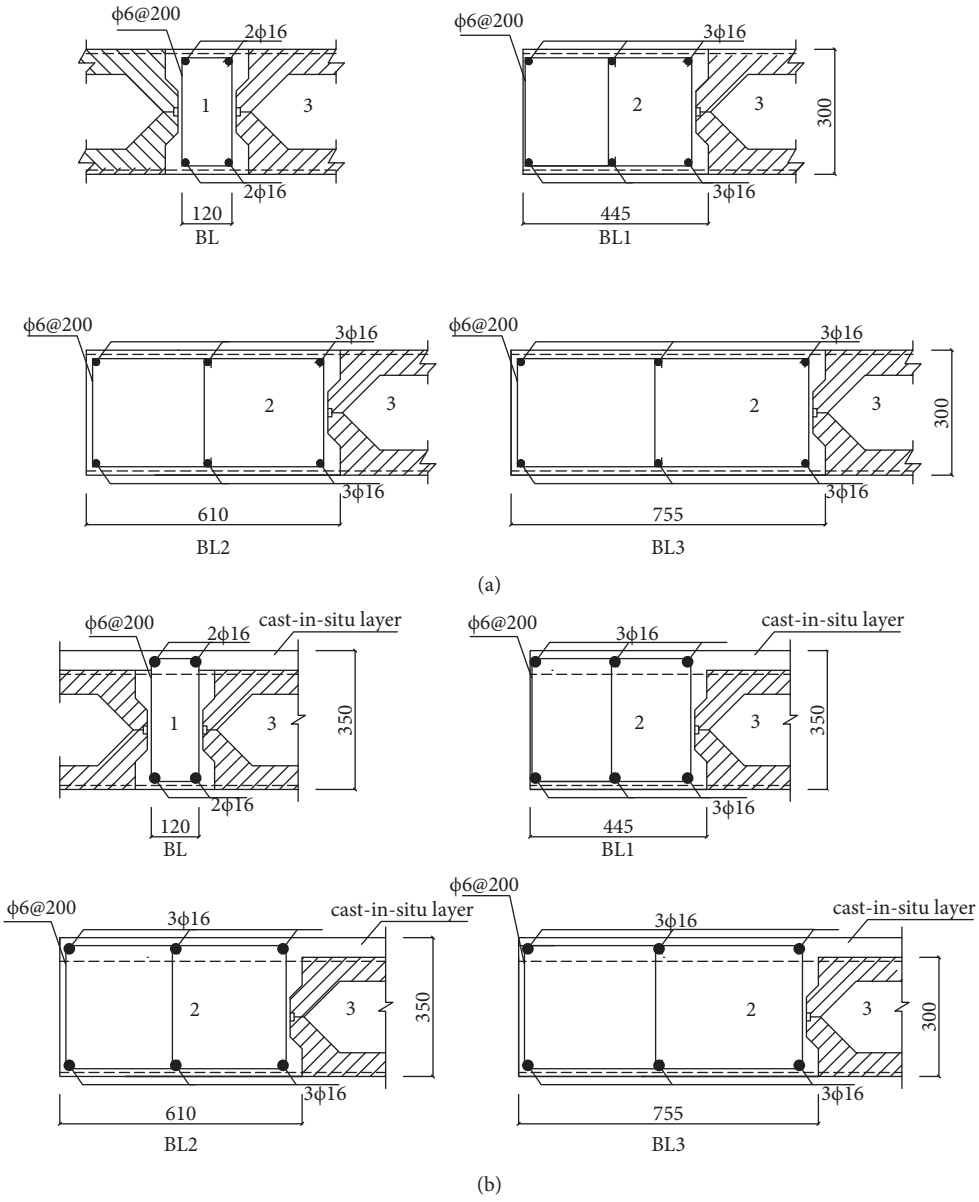

Figure 5: Specimen sketch map. (a) Open boxes. (b) Covered boxes. (1) Ribbed girder; (2) edge girder; (3) congruent box.

almost no damage, which could protect the ribbed girders effectively.

Some testing phenomenons observed during the second fire test were recorded as shown in Figure 7. The fire test process was similar to that mentioned above of the first fire test. At 15 min after ignition, the soleplates of some covered boxes began to generate surface spalling, leading to steel meshes within the soleplates being exposed to fire directly. At 40 min, some soleplates of covered boxes have been burned through, and four corners of the test slab began to deflect vertically upward. At 70 min, major cracks parallel to the ribbed girders appeared and developed quickly, and accordingly lots of water vapor escaped from the cracks. At 292 min, most soleplates of covered boxes were burned through. Although the covered boxes were not burnt through significantly, the furnace was switched off in account of the testing safety. Obviously, the covered box showed better fire resistance compared to the open box.

3.2. Instrumentation Stations. As shown in Figure 4, Type K thermocouples on the thermocouple trees T1–T6 were used to measure the concrete temperatures across the thickness of the slabs in each fire test. Two thermocouple trees named T1 and T2 were chosen to analyse the temperature distributions of ribbed girders and congruent boxes, respectively, because all the measure points received similar temperature data. Figure 8(a) shows the details of the layout of T1 and T2 in the first test slab. In T1 thermocouples, 1–7 were arranged to measure concrete temperatures of ribbed girders and the distance between them was 50 mm; likewise, thermocouples

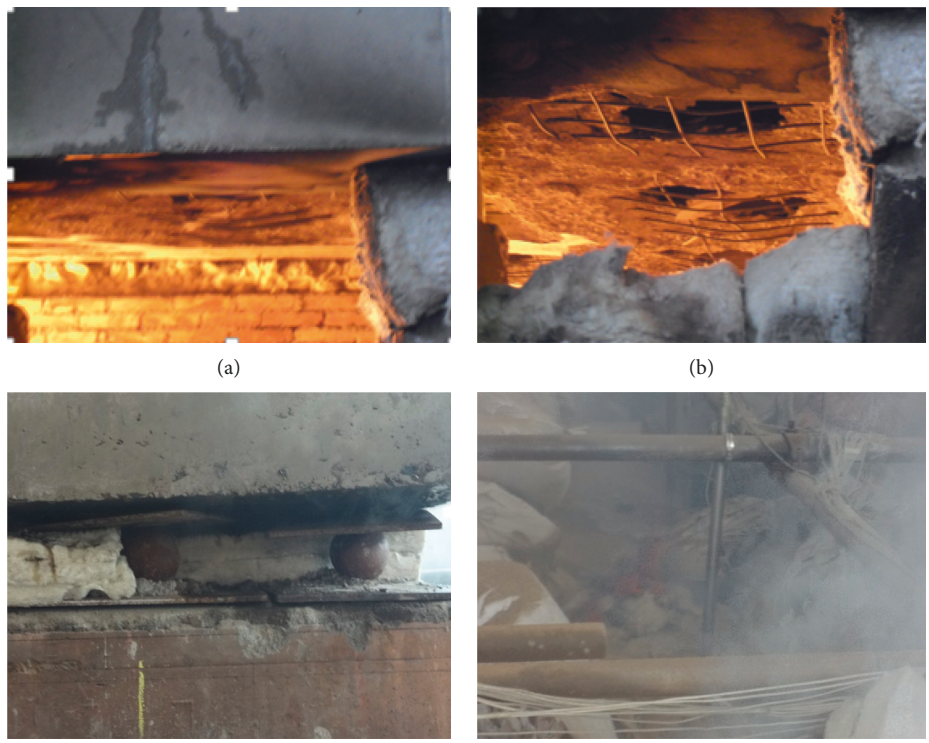

(a) (b)

(c) (d)

Figure 6: Fire test of the open box. (a) 5 minutes. (b) 15 minutes. (c) 35 minutes. (d) 69 minutes.

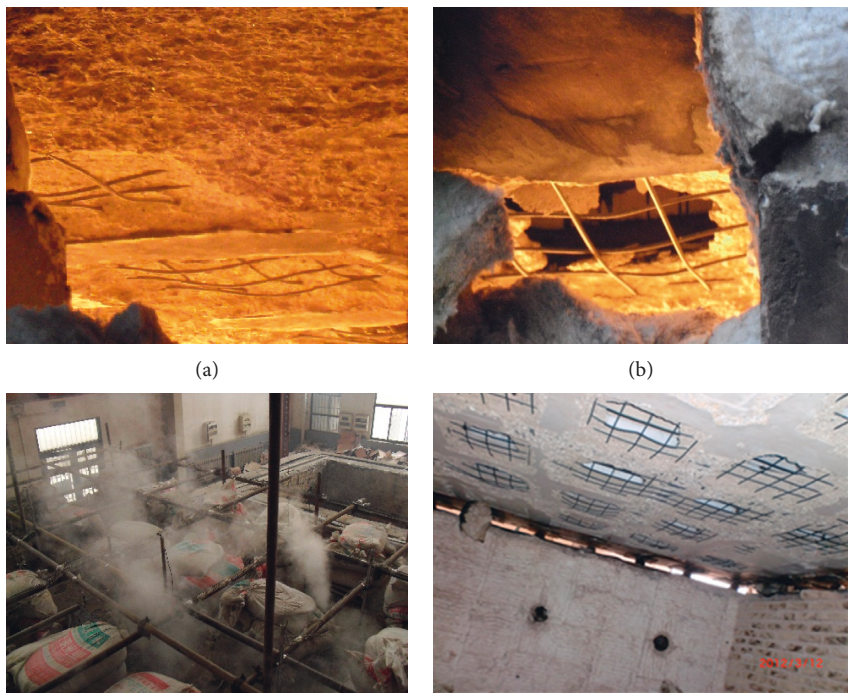

(a) (b)

(c) (d)

Figure 7: Fire test of the covered box. (a) 15 minutes. (b) 40 minutes. (c) 70 minutes. (d) 292 minutes.

8-9 were used to record the rebar temperatures. While in T2 thermocouples, 10–12 were settled to measure the temperatures of open boxes. Similarly, Figure 8(b) shows the details of the layout of the thermocouples in the second test slab. The major difference was that an additional thermocouple was arranged in thermocouple tree T1.

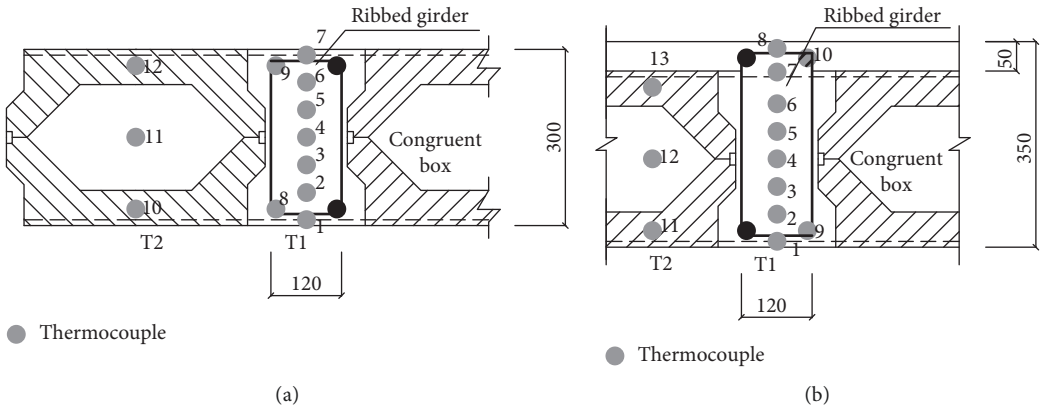

Figure 8: Arrangement of thermocouples. (a) Open box. (b) Covered box.

The vertical deflections of each AMH slab were measured during the fire tests. Figure 4 shows the positions of vertical LVDTs named W1~W3 whose limit travels ranged from 50 to 300 mm. The vertical deflections were measured across the center of the slabs in the long and short directions.

3.3. Gas Temperatures. During each fire test, four Type S thermocouples were used to monitor the furnace temperatures. As shown in Figure 9, the furnace temperature curves were obtained by averaging the temperatures recorded by the aforementioned four thermocouples. During the first fire test, the curve initiated a sharp rise and then continued to increase slowly until the furnace was shut off. The peak temperature at 90 min after ignition was 883°C. After the furnace was shut off, the gas temperature dropped quickly and the test concluded at 490 min after ignition. While during the second fire test, the curve indicated higher temperature and longer fire time compared to that of the first fire test. The maximum temperature at 292 min after ignition was 1120°C. Unfortunately, two burn nozzles were extinct from 23 min to 47 min after ignition, and thus during the time interval, the furnace temperatures dropped quickly. This, in turn, led to partial recovery of vertical displacements.

3.4. Temperatures of the Ribbed Girders. Except the furnace temperatures, Figure 9(a) also shows the temperatures of thermocouple tree T1 in the first fire test. The peak temperature at the bottom of ribbed girders was 883°C, but at other measure points their maximum temperatures were all less than 230°C. Apparently, the ribbed girders were protected effectively by the frame plates during the fire test. In other words, it seemed that only their bottom surface was exposed to fire. Meanwhile, Figure 9(a) indicates that temperatures of concrete measure points were approximately equal to those of the reinforcement measure points at the same depths. The maximum temperatures of the top and bottom reinforcing bars were 202°C and 62°C, respectively. Thus, during the fire test, temperatures of the reinforced bars remain low without significant strength loss [19]. Correspondingly, the ribbed girders could form a reliable framework, which maintained the load bearing function during the first fire test.

Similarly, Figure 9(b) shows the temperatures of thermocouple tree T1 in the second fire test. The fire exposure time and maximum furnace temperature significantly increased compared to that of the first fire test. The temperature curves of thermocouples 2–5 at the central part of the ribbed girders initiated a slow rise and then continued to increase sharply as the fire developed until the furnace was shut off. This was due to that the ribbed girders were changed gradually from a single surface subjected to fire to three surfaces subjected to fire as the fire test continued.

The temperatures at the upper parts of the ribbed girders showed a clear plateau during the temperature rise phase at about 100°C level due to evaporation of water. Additionally, after the furnace was shut off the temperatures at the upper parts continued to increase because heat conduction from the heated side to the unheated side held on as a result of temperature differentials. The aforementioned phenomenon also occurred during the heating of conventional reinforced concrete beams [20].

3.5. Temperatures of the Covered Boxes. As mentioned above, most of the soleplates of congruent boxes began to generate surface spalling and were burned through quickly at the early stage of the first fire test. The thermocouples embedded within the open box were found to be malfunctioning quickly after ignition; thus, complete temperature data were not recorded. In this paper, only the temperature data of the covered box were listed. Figure 10(a) shows the temperatures of thermocouple tree T2 plotted as a function of time under the condition that the soleplates were not burned through. It could be found that the temperature gradients increased slowly at the initial stage and then quickly after 100 min of the second fire test. The temperatures of the covered boxes showed a clear plateau during the temperature rise phase at about 100°C level due to evaporation of water. After the furnace was shut off, the temperatures at the bottom and top surfaces continued to increase because heat

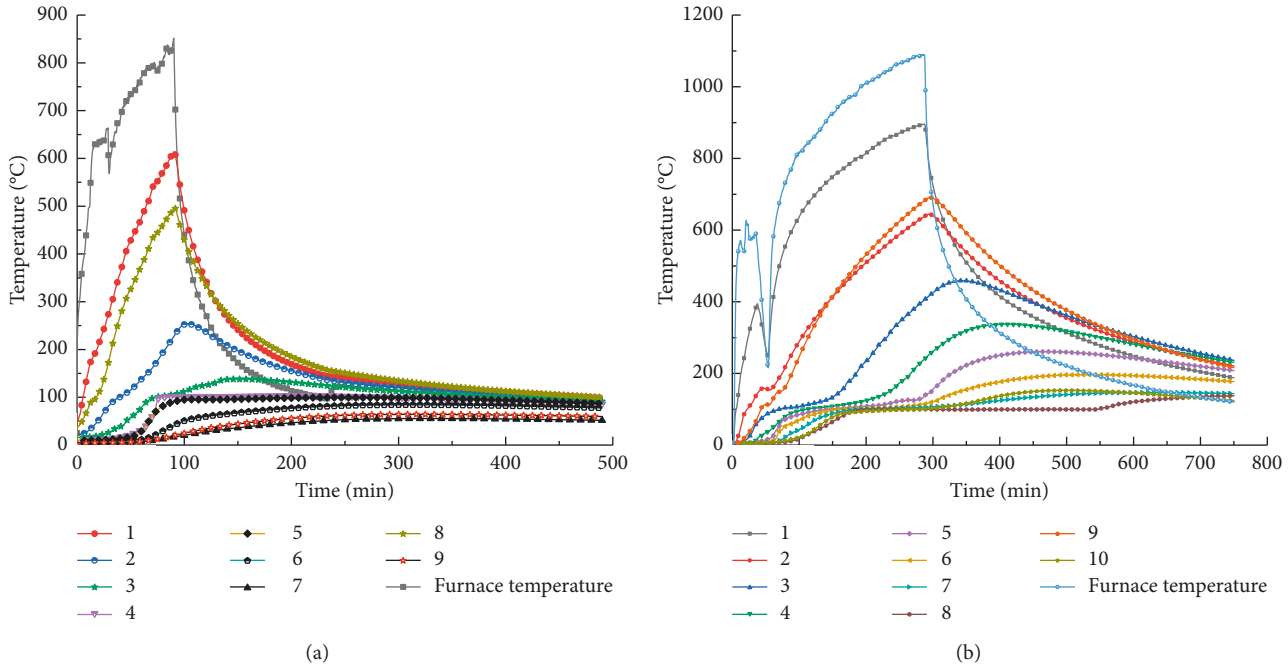

Figure 9: Temperature-time relationships of ribbed girders. (a) The first slab. (b) The second slab.

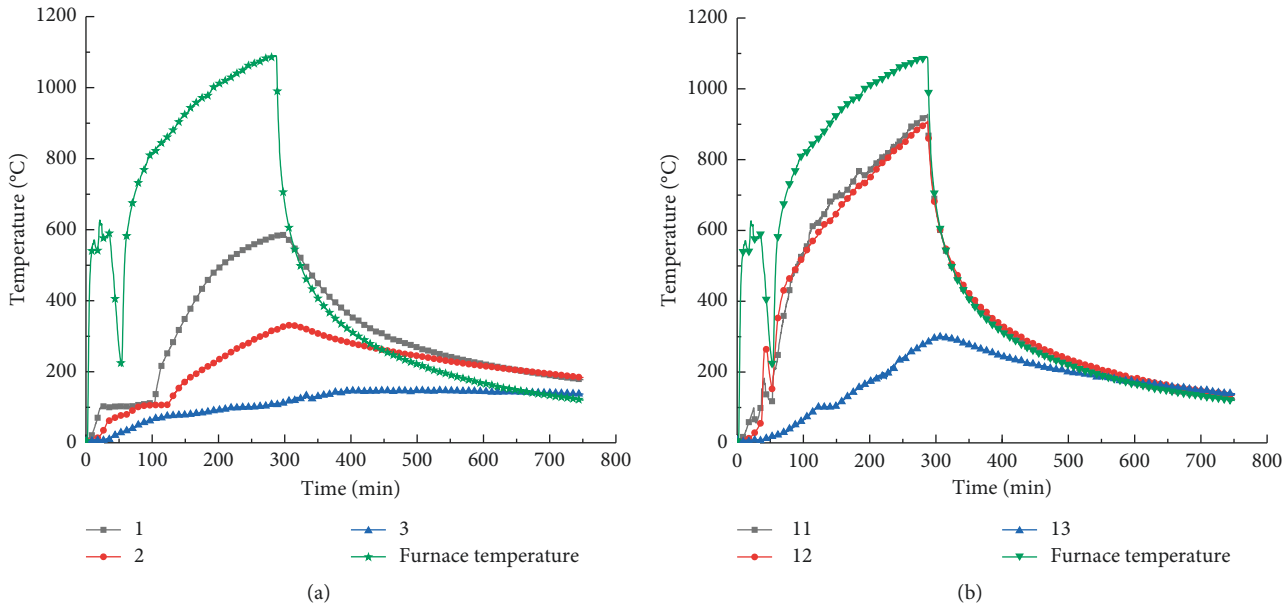

Figure 10: Temperature-time relationships of the covered boxes. (a) Without burn through. (b) Burn through.

conduction from the heated air within the covered boxes to the soleplates and top plates held on. Figure 10(b) shows the temperature changes of T2 under the condition that the soleplates were burned through. Apparently, temperatures of air within the covered boxes and their soleplates were basically the same and obviously higher than those of the covered boxes which were not burned through. Therefore, avoiding premature explosion of covered boxes was crucial to improve the fire resistance of the AMH slab.

3.6. Deflection Analysis. Figure 11(a) shows the variation of the vertical displacements of the first test slab plotted against time during the heat-up and cool-down phase. In the heating stage, the displacement changed approximately linearly with time, and the main reasons were as follows: firstly, as the fire continued, the mechanical properties of the first slab deteriorated gradually; additionally, the soleplates of the open boxes had surface spalling and fall off quickly after ignition, which further led to stiffness degradation; thus the vertical deformation

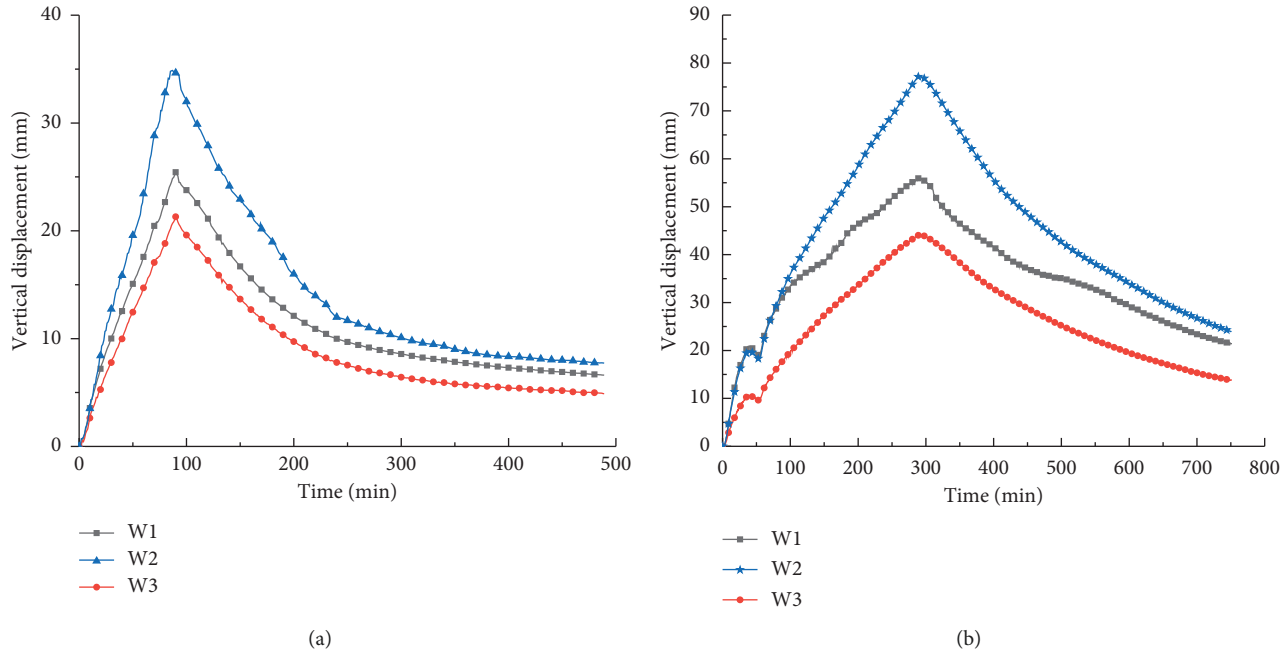

Figure 11: Vertical deflections-time relationship. (a) The first fire test slab. (b) The second fire test slab.

increased gradually; secondly, as the soleplates were burned through and exited the work, the structural system transformed into the ribbed floor system, which postponed the high temperature deformation. The maximum displacement reached 37.5 mm at the furnace shut-off point. In the meantime, the four simply supported edges of the AMH slab were supported by steel balls or rollers on reinforced concrete furnace walls without in-plane constraints, and the four corners were not clamped; thus, the curves did not present displacement platform or mutation phenomenon [13, 15]. After the furnace was shut off, the displacements gradually recovered and the residual displacements were approximately 6 mm at the end of the test. Obviously, the AMH slab showed strong displacement restoring capacity after cooling.

Figure 11(b) shows the vertical displacements of the second test slab plotted as a function of time. The curves showed similar displacement changes compared to those of the first slab, but the second test slab showed higher temperatures and greater displacements. Unfortunately, two burn nozzles were extinct from 40 min to 60 min after ignition, and thus during the time interval, the furnace temperature dropped quickly. This, in turn, led to partial recovery of vertical displacements. After the furnace was shut off, the displacements continued to increase slightly and then decrease rapidly; this was due to heat conduction from air within the covered boxes to the covered boxes, and thus the fire failure might appear during the cooling phase [13]. The maximum displacement recorded at its central point was 77.2 mm, and the residual displacement after termination was 24 mm. The recovery ratio was about 70%, which was much better than that of the conventional reinforced concrete slabs (35.2%) [11, 21].

4. Fire Resistance Analysis and Discussion

The two AMH slab tests under fire indicated that the covered box has better fire resistance compared to the open box; thus, the covered box is recommended to adopt in structural fire-resistant design. Up to now, Chinese fire resistance classes of building components and constructions are always determined according to a time limit of simply supported solid slabs during the standardized fire test. Detailed, architectural fire proof grades can be classified into four grades, and the floor slab in each architectural fire proof grade has a time limit in minutes 90, 60, 30, and 15, respectively. As a new structure, the AMH slab has no rational failure criterion yet. In this paper, the fire failure criterion of conventional reinforced slabs is adopted to discuss the fire resistance of the AMH slab. It is assumed that the designed fire resistance class of the AMH slab in the standard is 90 min, and the corresponding peak temperature is 1006°C. Although the actual temperature-time curves greatly deviated from the standard ISO834 curve and the heating rate was relatively slow, it can be adopted to study the fire resistance of the AMH slab with partial safety. During the real fire test, it took 196 min to reach the aforementioned peak temperature (1006°C) and the corresponding midspan displacement was 57.2 mm, less than $L^2/400\,d$ (101 mm); thus, the load-bearing function of the AMH slab was maintained during the equivalent fire exposure time. During the second fire test, the covered boxes were not burned through although most soleplates have been burned through since 40 min after ignition, so the integrity was also maintained. At 196 min after ignition, the average temperature rise over the whole of the nonexposed surface was 125°C and the maximum temperature rise was 175°C. Thus, its insulation also satisfied the specification requirements [22].

Although the fire resistance of the AMH slab consisting of covered boxes meet the regulatory requirements, its serviceability limit state was seriously affected because most soleplates had surface spalling and fall off. One reason was material degeneration due to elevated temperature, and the other reason was that some concrete mixed water entered the congruent boxes during construction. As the water gradually vaporized, the steam pressure within congruent boxes increased sharply. Thus, some soleplates began to generate surface spalling quickly and were burned through at 40 min after ignition. At the meantime, some well-sealed congruent boxes only had surface spalling and were not burned through during the fire test. Therefore, the sealing quality of congruent boxes has a great influence on their fire resistance. In view of concrete vibration, which is necessary to consolidate concrete and reduce the amount of air within the concrete, it is very difficult to keep the sealing capacity of congruent boxes under construction. Thus, additional measures should be taken to meet the requirements of fire resistance and service function of the AMH slab. Generally, improving the manufacturing technique of congruent boxes, adding concrete protective layer, or spraying fireproofing coating at the bottom of the AMH slab can be chosen to fulfill the aforementioned dual requirements.

Generally, the manufacturing technique of congruent boxes includes prefabrication and assembly of the subcomponents. During the prefabrication, stricter production standards should be implemented; moreover, during the assembly expansive water-proof strips can be adopted to improve the seal quality. However, additional measures are still needed to meet the fire resistance and service function of the AMH slab. Adding concrete protective layer at the bottom of the AMH slab is low in material, but the structural construction between the concrete protective layer and the soleplates of congruent boxes is complex and difficult. Furthermore, the suitable thickness of the concrete protective layer should be determined to avoid explosive spalling of the AMH slab. Applying fire-retardant coatings is simple and has little effect on the clearance height. Wu and Zhou [23] suggested that the nonexpandable fire-retardant coating with a thickness of 15–20 mm can suppress the high-temperature spalling effectively. Additionally, fire-retardant coatings can obviously reduce the temperature of the soleplates of congruent boxes. In the follow-up study, suitable thickness of the coating needs to be determined according to the fire rating of the AMH slab.

5. Conclusions

Two fire tests were conducted on two AMH slabs consisting of the open box and the covered box, respectively, with four-edge simple supports under the combined effects of constant loading and fire. The relevant test conclusions on gas temperatures, temperature distribution of ribbed girders and congruent boxes, vertical deflections, and failure criteria were presented and discussed in detail. Several general conclusions can be summarized as follows:

(1) During the fire tests, the close box showed much better fire resistance compared to the open box; thus, the covered box was recommended to adopt in structural fire-resistant design.

(2) As the soleplates were burned through and exited the work, the AMH slab was transformed into the ribbed floor system, which postponed the high temperature deformation.

(3) The sealing quality of congruent boxes has a great influence on the fire resistance of the AMH slab.

(4) As a new type of floor system, the AMH slab needs further optimum design to meet its requirements of fire resistance and service function.

Data Availability

The research data used to support the findings of this study are available from the corresponding author upon request. At present, we are conducting finite element analysis of the assembled monolithic hollow-ribbed slabs under fire; thus, the data cannot be open now.

Conflicts of Interest

The authors declare that they have no conflicts of interest.

Acknowledgments

The authors are very grateful to Professor Zhao, Shandong Jianzhu University, for his encouraging supervision and support for this work. This work was supported by the NSFC (Grant no. 51768017) and Hainan Province Natural Science Fund (Grant no. 20165189). The authors gratefully appreciate the support.

References

[1] Z. Y. Qiu, *Cast-In-Situ Hollow Concrete Floor*, pp. 1-2, China Building Industry Press, Beijing, China, 2007.

[2] J. Li, *Experimental research and analysis on static and fatigue performance of the assembled monolithic hollow-ribbed floor*, Ph.D. thesis, Hunan University, Changsha, China, 2016.

[3] K. Z. Zhao, Z. R. Li, and L. Wang, "Experimental study on mechanical performance of assembly box concrete hollow floor structure with assembly style," *Engineering Mechanics*, vol. 28, no. 1, pp. 145–150, 2011.

[4] X. H. Zhou, W. Chen, and F. B. Wu, "Study on stiffness of assembled monolithic concrete hollow floor with two-way ribs," *Journal of Building Structures*, vol. 32, no. 9, pp. 75–83, 2011.

[5] P. S. Shen and J. H. Zhu, "Theoretical and experimental research on calculating methods for ultimate load and deflection of four sides simply supported RC waffle floor slab," *China Civil Engineering Journal*, vol. 36, no. 8, pp. 7–11, 2003.

[6] K. M. Mosalam and C. J. Naito, "Seismic evaluation of gravity-load-designed column-grid system," *Journal of Structural Engineering*, vol. 128, no. 2, pp. 160–168, 2002.

[7] C. Q. Howard and C. H. Hansen, "Vibration analysis of waffle floors," *Computers & Structures*, vol. 81, no. 1, pp. 15–26, 2003.

[8] G. A. Jimenez, "Assessment and restoration of post-tensioned waffle slabs," in *Proceedings of the Structure Congress 2010*,

pp. 1074–1081, American Society of Civil Engineers (ASCE), Orlando, FL, USA, May 2010.

[9] d. S. M. d. S. Shirley, A. E. M. S. Ibrahim, and d. C. D. S. Lidia, "Shear resistance of reinforced concrete waffle flat slabs around the solid panel," *Materials and Structures*, vol. 49, no. 4, pp. 1367–1380, 2016.

[10] C. G. Bailey and W. S. Toh, "Small-scale concrete slab tests at ambient and elevated temperatures," *Engineering Structures*, vol. 29, no. 10, pp. 2775–2791, 2007.

[11] Y. L. Dong and C. J. Zhu, "Limit load carrying capacity of two-way slabs with two edges clamped and two edges simply supported in fire," *Journal of Structural Engineering*, vol. 137, no. 10, pp. 1182–1192, 2011.

[12] P. J. Moss, R. P. Dhakal, G. Wang, and A. H. Buchanan, "The fire behavior of multi-bay, two-way reinforced concrete slabs," *Engineering Structures*, vol. 30, no. 12, pp. 3566–3573, 2008.

[13] B. Li, Y.-L. Dong, and D.-S. Zhang, "Fire behaviour of continuous reinforced concrete slabs in a full-scale multi-storey steel-framed building," *Fire Safety Journal*, vol. 71, pp. 226–237, 2015.

[14] Z. N. Yang, Y. L. Dong, and W. J. Xu, "Fire tests on two-way concrete slabs in a full-scale multi-storey steel-framed building," *Fire Safety Journal*, vol. 58, pp. 38–48, 2013.

[15] Y. Wang, Y.-L. Dong, B. Li, and G.-C. Zhou, "A fire test on continuous reinforced concrete slabs in a full-scale multi-story steel-framed building," *Fire Safety Journal*, vol. 61, pp. 232–242, 2013.

[16] D. Kakogiannis, F. Pascualena, B. Reymen et al., "Blast performance of reinforced concrete hollow core slabs in combination with fire: numerical and experimental assessment," *Fire Safety Journal*, vol. 57, pp. 69–82, 2013.

[17] *Load Code for the Design of Building Structures*, China Building Industry Press, Beijing, China, 2012.

[18] *Code of Design on Building Fire Protection and Prevention*, China Building Industry Press, Beijing, China, 2018.

[19] *Eurocode 3: Design of Steel Structures. Part 1.2: General Rules-Structural Fire Design*, Commission of the European Communities, Brussels, Belgium, 2003.

[20] V. K. R. Kodur and M. Dwaikat, "A numerical model for predicting the fire resistance of reinforced concrete beams," *Cement and Concrete Composites*, vol. 30, no. 5, pp. 431–443, 2008.

[21] L. Lim, A. Buchanan, P. Moss, and J.-M. Franssen, "Numerical modelling of two-way reinforced concrete slabs in fire," *Engineering Structures*, vol. 26, no. 8, pp. 1081–1091, 2004.

[22] *Fire-Resistance Tests-Elements of Building Construction-Part 1: General Requirements*, China Standards Press, Beijing, China, 2008.

[23] B. Wu and P. Zhou, "Explosive spalling of high strength concrete coated with fire retardation coating at high temperatures," *Journal of Building Materials*, vol. 14, no. 3, pp. 406–412, 2011.